Essential Readings in Light Metals: Aluminum Reduction Technology.
Edited by Geoff Bearne, Marc Dupuis and Gary Tarcy.

COMPARISON OF VARIOUS METHODS FOR MODELING THE METAL-BATH INTERFACE

Dagoberto S. Severo[1], Vanderlei Gusberti[1], André F. Schneider[1], Elton C. V. Pinto[1], Vinko Potocnik[2]

[1] PCE Engenharia S/S Ltda, Rua Caeté 162, Porto Alegre, RS, Brazil – E-mail: pce@pce.com.br
[2] Vinko Potocnik Consultant, 2197 rue de Régina, Jonquière, Québec, Canada, G7S 3C7

Keywords: Aluminum reduction, Magnetohydrodynamics, Metal-bath interface, Numerical simulation

Abstract

The correct evaluation of the stationary metal-bath interface in aluminum reduction cells is still a source of discussion and controversy. The objective of this paper is to present some calculations of the interface performed by different methods, used in software packages and to compare them with measured metal-bath interface profile in a real cell. Our comparison includes Shallow Layer approach and 3D multiphase methods, such as: homogeneous and inhomogeneous volume of fluid (VOF) as well as floating grid method. Different boundary conditions on the top of bath channels are tested in VOF methods. Finally, a simple generic magnetic field and vertical current density are proposed for software benchmarking of this problem.

Introduction

In the aluminum reduction cells, widely known as Hall-Héroult cells, the electrochemical reduction occurs inside the liquid electrolyte layer (bath), which is floating on top of the liquid metal due to density difference. This is a two-phase system of immiscible liquids. If only the gravity force is present, the metal-bath interface is flat and horizontal. However, in an operating cell, the combination of the electric current and the magnetic field gives volumetric forces, known as Lorentz or electromagnetic forces. These are responsible for the metal and bath flow as well as for the metal-bath interface deformation.

The shape of the stationary metal-bath interface is a very important parameter in cell behavior and operation. The anode setting height is influenced by the interface shape. A long time ago, it was already reported by Givry [1] that cells with flatter interface are more stable and easier to operate.

Measuring the metal-bath interface accurately in operating cell is a challenge. In this paper, we use the measured metal-bath interface heights published by da Mota [4], which were made by measuring the anode slope after anode changing in eight cells. We use these measurements for model validation.

The first attempts to calculate stationary bath-metal interface shape were made by Givry [1, 2]. In his paper [2], Givry discussed the influence of side channels on the interface shape. It was shown that the interface shape is a function of hydraulic resistance of the channels, which must be taken into account for correct evaluation of interface shape. Moreau and Evans [3] published a shallow layer method for the calculation of the steady state metal and bath flow and the metal-bath interface shape. They also included the influence of the channels. Later on, fully three-dimensional models were developed, using commercial software packages ESTER/PHOENICS (henceforth called ESTER) [5, 6] and Ansys CFX [7]. In ESTER the metal-bath interface is calculated using floating grid method in which the grid plane of the metal bath interface floats on the deforming interface and all other grid lines in the metal and in the bath stretch or compress proportionally to the vertical deformation of the interface. In the Ansys CFX model, one of the Volume of Fluid (VOF) methods available in the package is used. Some difficulties with VOF method will be discussed in this paper.

Shallow layer approach is still popular for in-house and academic models [8]. This approach has the advantage of not using a vertical mesh and is therefore computationally very rapid. In 3D, the floating grid approach is also very rapid; it can use a rough grid in the vertical direction because the interface is always sharply defined by the vertical position of the interface grid which is calculated from the pressure boundary condition at the interface. On the other hand, in the 3D VOF methods, the vertical direction must be well refined in order to represent the interface properly. Moreover, the steady state in VOF methods is obtained by a transient calculation; which makes the method very computationally intensive.

There is no agreement in the literature which method of the metal-bath interface calculation is the best. In this work, a few methods are compared for the same situation in order to help understanding the problem and to clarify the necessary procedures to be followed to obtain correct results.

First, a simple interface calculation is proposed. Bath and metal inside a rectangular box are subjected to a linear force density. This is a hydrostatic problem which the models should be able to calculate easily.

In the second part of the paper, a real cell is calculated by different methods and the results are compared with the reference measurements [4], which were made in a modified AP13 cell at ALBRAS.

Finally an analytical expression for magnetic field and current density are proposed for benchmark tests of the models. The shape of these functions is similar to the one found in real cells.

Analytical Solution in a Rectangular Box

The rectangular box has dimensions comparable with real cells as shown in Figure 1:

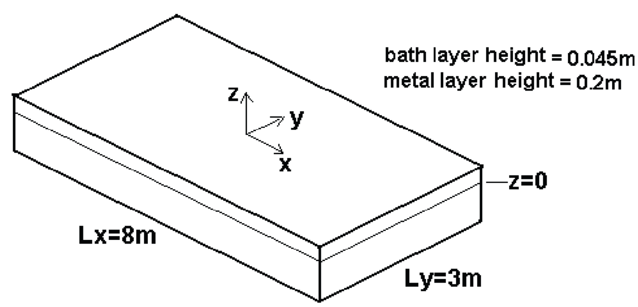

Figure 1: Box dimensions used in analytical solution and coordinate system.

The top of the box is open and a force density $F(x) = -25x$ N/m³ is applied only in the metal. Note that the distribution does not depend on y and z direction. Bath and metal densities are 2070 and 2270 kg/m^3, respectively. The acceleration of gravity is vertical and equal to 9.81 m/s^2. This force field is irrotational and from hydrostatics we obtain the vertical interface displacement:

$$h(x) = -0.00637x^2 + 0.03398 \tag{1}$$

The difference between maximum and minimum interface height over the length of the box is 0.10194 m. This value is taken as the base of comparison between models.

Shallow Layer Model

A shallow layer model was developed at PCE to perform quick steady state flow and interface calculations. It solves the Navier-Stokes equations (simplified for shallow layer approach) in the metal and the bath. The interface deformation is obtained following the Moreau and Evans approach [3] which considers pressure difference between the two layers and the geometry of the channels. The agreement with the analytical solution is perfect. The difference between maximum and minimum interface height is 0.10197 m, which differs from the analytic solution only by 0.03%.

Ansys CFX Model (2-phase Homogeneous)

Ansys CFX free surface modeling uses a pseudo-VOF formulation to compute multiphase flow and interface tracking. It requires small vertical mesh spacing. In the homogeneous model, one single bulk velocity field is computed for the whole domain, with each fluid region having its proper density. According to the CFX Manuals [9], this method gives good results when the density difference between fluids is sufficiently high to avoid entrainment. The interface location is calculated where the volume fraction of the metal and of the bath is 0.5.
The difference between maximum and minimum interface height is 0.10210 m, which represents an error of 0.16%.

Ansys CFX Model (2-phase Inhomogeneous)

In the inhomogeneous model, two velocity fields are calculated for the whole domain: one for the metal and one for the bath, even in the regions of pure bath or pure metal. The mesh size and quality must be carefully chosen in order to keep enough accuracy. As in the homogeneous model, the interface location is calculated where the volume fraction of the metal and of the bath is 0.5.
The difference between maximum and minimum interface height is 0.10014 m, with an error of 1.77% with respect to the analytical solution.

Ansys CFX Model (3-phase)

For the complete analysis of the open box problem, it might be necessary to consider also the air-bath interface. In the 2-phase pseudo-VOF calculations, bath can flow in and out of the domain, without any information on the domain outside. In the 3-phase calculation, air is included, which limits bath movement. Again, the interface location is calculated where the volume fraction of the metal and of the bath is 0.5.
The difference between maximum and minimum interface height is 0.10194 m with an error of 0.51% with respect to the analytical solution. The 3-phase model introduces another difficulty: the interface air-bath is also calculated, and its position affects the metal-bath interface. In the cell, the air-bath interface deformation is expected to be around 10 times smaller than the metal-bath interface deformation. The mesh needs to be fine in the vertical direction to catch both interfaces.

Discussion: Analytic Case Study in ANSYS CFX

The deformation of the metal-bath interface in the open box with hydrostatic forces is calculated well with Ansys CFX 2-phase and 3-phase homogeneous model. The comparison of all model results with the analytical solution is shown in Figure 2.

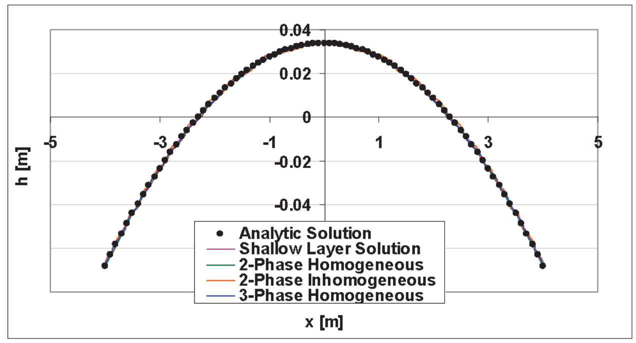

Figure 2: Rectangular box solution obtained by the models (lines) compared with the analytical solution (black dots)

It can be concluded that different models tested successfully described the simple analytical model. However, a real cell contains more difficulties such as: channels and background flow caused by complex electromagnetic force fields. In the cell, electromagnetic forces are applied in both liquid layers and the force difference between the layers is the major influence in the interface displacement.

Calculations for a Real Cell with Measurements

Here we used the models to calculate the static interface for the modified AP13 at ALBRAS and compare the results with the measurements published by da Mota [4].
All the calculations were done using constant eddy viscosity for bath and metal, except in one case where the k-epsilon (k-ε) turbulence model was used. Table 1 gives the eddy viscosity used in the models, adjusted so that the calculated interface heights and velocities agreed with the measured ones. The velocity measurements with iron rod method are shown in the Figure 3. We are still investigating why ESTER version 5.2 used in this research needs much higher viscosities than an earlier version used in a previous paper [10], where they were in the range of 0.5 - 1.0 Pas.

Table 1 Eddy viscosity (Pa.s) for different models

	metal	bath
Shallow Layer*	0.6	0.7
ESTER	4.2	23.1
Ansys CFX	0.6	3.3

**In the Shallow Layer a vertical friction coefficient of 6.0 was used.*

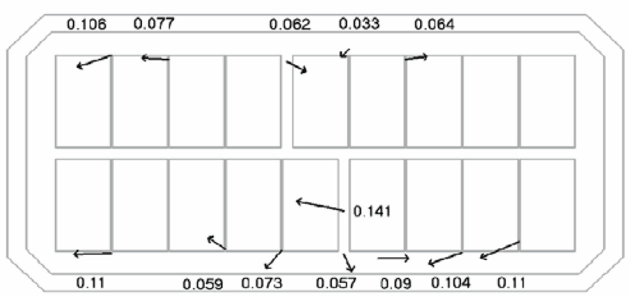

Figure 3: ALBRAS metal velocity measurements (m/s)

Shallow Layer Model

Figure 4 and Figure 5 show the results obtained by the Shallow Layer model. They are in very good agreement with the measured interface profile. In Figures 5, 7 and 8, the upstream and downstream curves of the calculated results were taken at the middle of the upstream and downstream anodes, considering that the measured values were obtained by the measurement of consumed anode slopes.

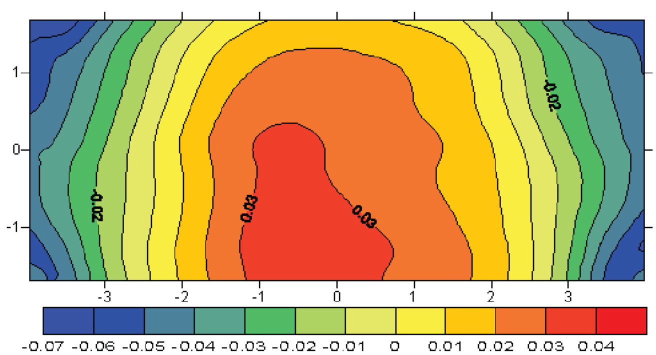

Figure 4: Metal-bath interface shape (m) obtained by the Shallow Layer model for the modified AP13 cell.

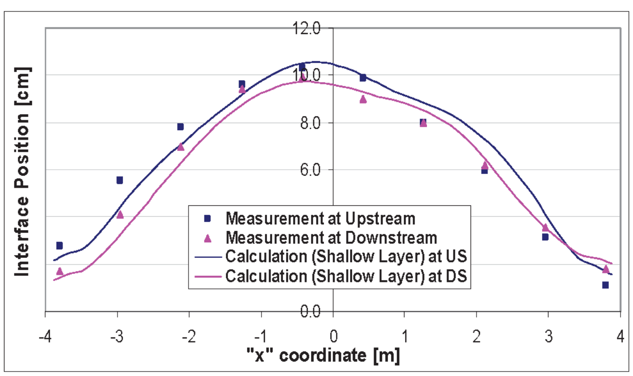

Figure 5: Metal-bath interface shape, calculated by Shallow Layer model versus measured by ALBRAS.

ESTER Model:

The calculation domain in public ESTER includes metal pool, bath and anodes up to the top of the anode carbon. Boundary conditions are: vertical current density distribution at the bottom of the metal pad and a specified voltage at the top of the anodes. In order to make the comparisons on the same basis, we used the same vertical current density at the bottom of the metal pad and the same magnetic field distribution in the metal and the bath for all the models. Figures 6 and 7 give ESTER results. These are also in very good agreement with the measurements. ESTER deviations from the measurements are similar to the Shallow Layer ones: in both, the calculated upstream curve appears slightly shifted to the right of the measurements and the downstream curve follows about 1 cm below the measurements on the left-hand side of the graph only. The difference between maximum and minimum deformation of the interface is equal in both models and in the measurements.

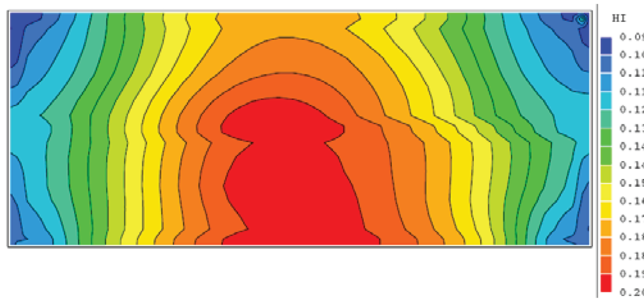

Figure 6: Metal-bath interface shape (m) obtained by ESTER model for the modified AP13 cell.

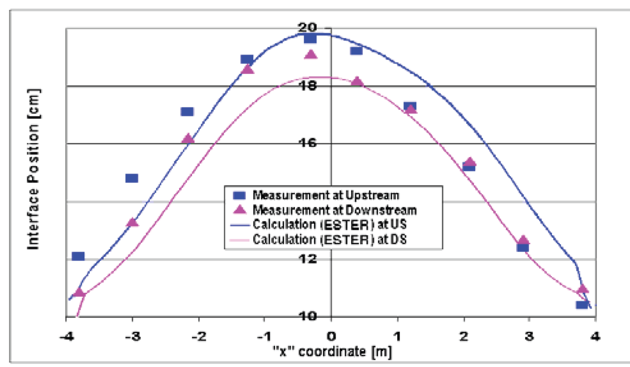

Figure 7: Metal-bath interface shape, calculated by ESTER model versus measured.

Ansys CFX Model (2-phase Homogeneous): Open Channels

Figure below shows the results obtained by the 2-phase Homogeneous model. The top of the channels is considered as open surface. The calculations overestimate the total interface displacement in comparison with the measured interface profile.

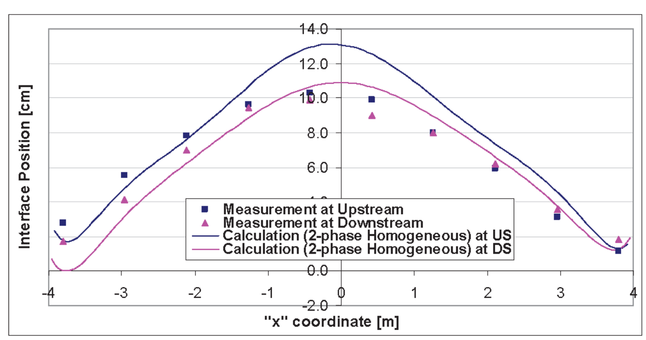

Figure 8: Metal-bath interface shape, calculated by CFX 2-phase Homogeneous model versus measured.

Ansys CFX Model (2-phase Homogeneous): Closed Channels

One could argue that the real cell is almost a closed system because the area of the channels is smaller than the anode shadow. A fully closed system model is an approximation. We performed a closed system 2-phase calculation and the result is not satisfactory at all, as shown in Figure 9.

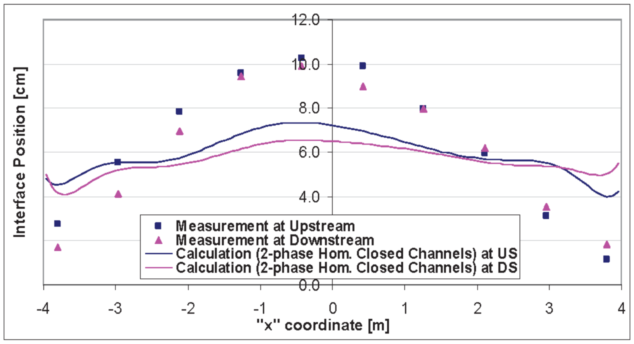

Figure 9: Metal-bath interface shape, calculated by CFX 2-phase Homogeneous model (closed channels) versus measured.

Figure 9 clearly shows that it is necessary to include the open channels. Their influence is determinant for a good interface shape calculation.

Ansys CFX Model (3-phase)

The 3-phase model which considers the aluminum-bath-air system was calculated and the results are shown in the Figure 10 and Figure 11.

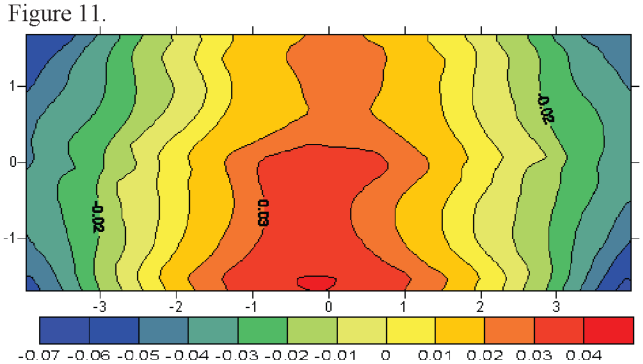

Figure 10: Metal-bath interface shape (m) obtained by the CFX 3-phase Homogeneous model for the modified AP13

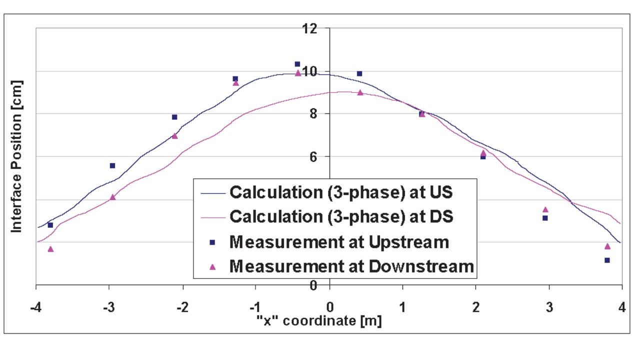

Figure 11: Metal-bath interface shape, calculated by CFX 3-phase Homogeneous model versus measured.

The results show the need of including 3-phase physics in the calculation in order to achieve correct interface description with Ansys CFX.

Ansys CFX Model (3-phase, k-ε Turbulence Model)

It has been reported [7, 10] that the standard k-ε turbulence model does not describe well the physics of the MHD present in the cell. Figure 12 shows the result of the 3-phase modeling using k-ε turbulence model compared with measurements.

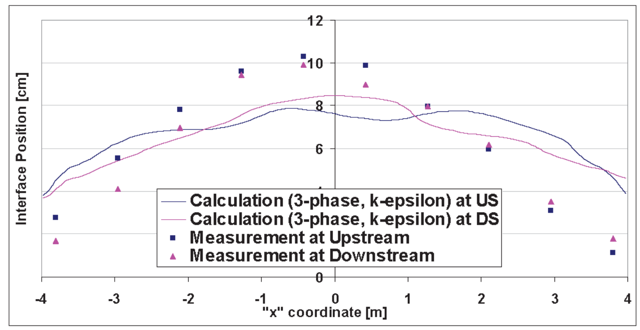

Figure 12: Metal-bath interface shape, calculated by CFX 3-phase Homogeneous model (k-ε turbulence model) versus measured.

The k-ε model fails to track the interface correctly. According to the literature [9, 11, 12], there are many situations where two-equation turbulence models should not be used. These situations include rotating flows and flows dominated by body forces, which are characteristics of metal and bath circulation. In our opinion, these features are the reason for k-ε turbulence model failure. Figure 13 shows the interface deformation obtained using the k-ε turbulence model and its relationship with calculated metal flow. The pool centers seem to cause an exaggerated depression at the interface.

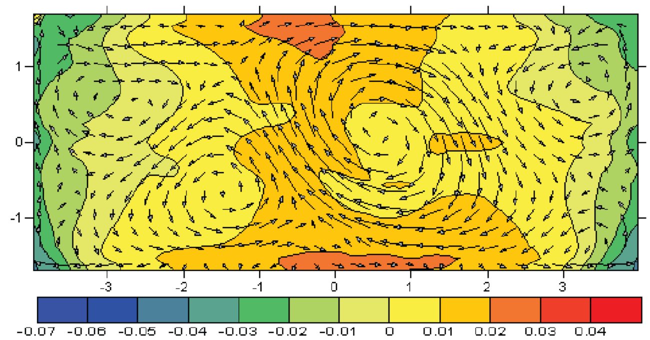

Figure 13: Interface deformation (m) obtained by the 3-phase k-ε turbulence model (metal velocity vectors in black)

Benchmark Magnetic and Electric Fields for Software Testing

The proposed benchmark magnetic field and current density distributions are simple analytical expressions, but their shape and magnitude are typical for real cells. Cell dimensions are L_x = 8 m, L_y = 3 m. The coordinate system is the same as in the analytical example (origin at the cell center). ACD = 0.045 m, metal height = 0.2 m, bath height = 0.18 m, metal density = 2270 kg/m^3, bath density = 2070 kg/m^3. The width of the center, sidewall and endwall channels is 0.15 m. For simplicity, no inter-anode gaps in the longitudinal direction are used.

For the current density calculations, the current density at the top of the cathode block in [A/m^2], is specified as the boundary condition:

$$j_z = -5625 - 2500y^2 \tag{2}$$

The three components of current density inside bath and metal can be calculated using constant current density at the bottom of anodes. In ESTER the electrical potential is specified at the top of anode blocks.

The three components of the magnetic field inside the bath and the metal, in [mT], are:

$$B_x = 6.0y \tag{3}$$

$$B_y = -3.0x + 1.5 \tag{4}$$

$$B_z = 1.0xy + 0.5 \tag{5}$$

The resulting force density field is obtained as vector product of electric current density and magnetic field.

All the models, except ESTER, used constant eddy viscosity for bath and metal as presented in Table 1. In ESTER the viscosities for the benchmark case were 86% of the values in Table 1.

Shallow Layer Model

The interface deformation and the metal flow obtained by the Shallow Layer method are shown in Figure 14 and Figure 15, respectively.

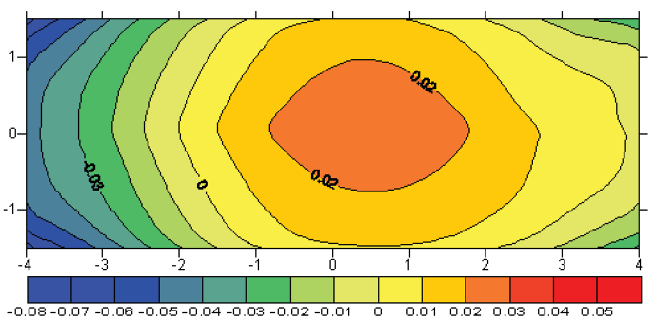

Figure 14: Metal-bath interface deformation (m) obtained by the Shallow Layer method for the benchmark case

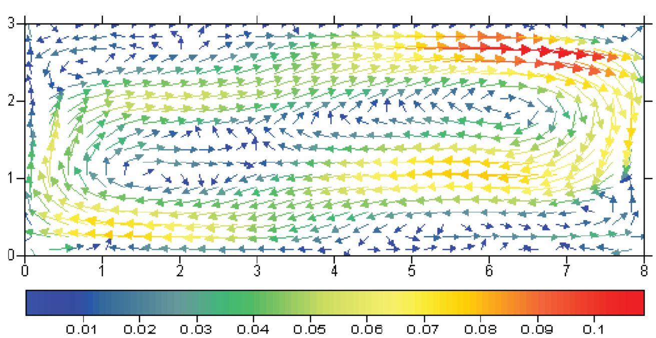

Figure 15: Metal flow (m/s) obtained by the Shallow Layer method for the benchmark case

ESTER Model

The interface deformation and the metal flow are shown in Figures 15 and 16, respectively.

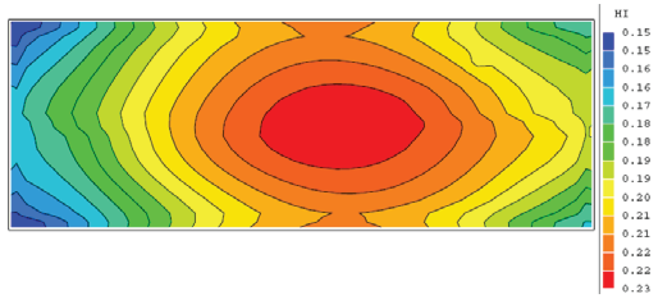

Figure 16: Metal-bath interface deformation (m) obtained by ESTER for the benchmark.

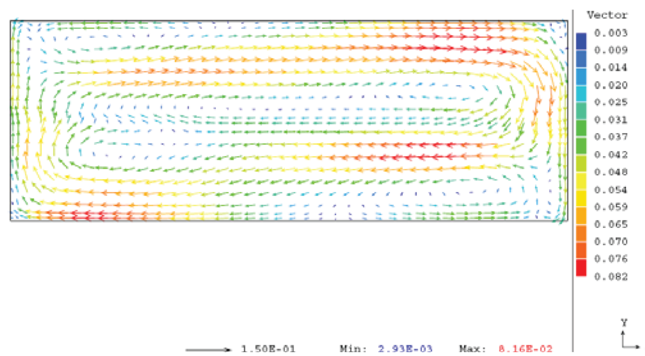

Figure 17: Metal flow (m/s) obtained by ESTER for the benchmark.

Ansys CFX Model (3-phase)

The interface deformation obtained by three-dimensional 3-phase model is shown in the Figure 18. Velocity vectors are shown in Figure 19.

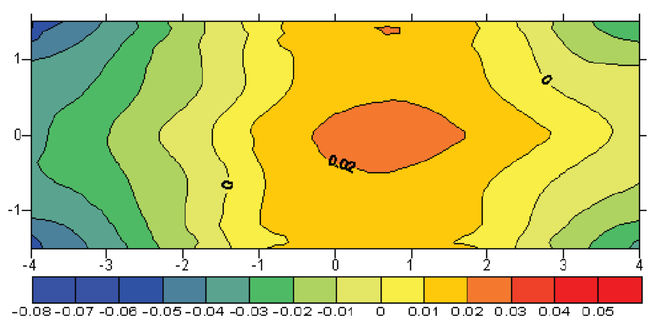

Figure 18: Metal-bath interface deformation (m) obtained by the Ansys CFX 3-phase model for the benchmark case

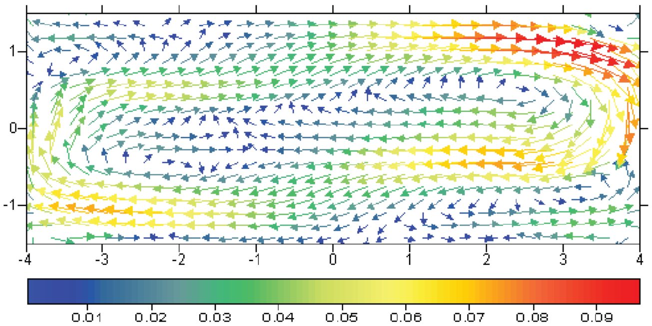

Figure 19: Metal flow (m/s) obtained by the Ansys CFX 3-phase model for the benchmark case

Interface profile on the longitudinal axis located at the center of the cell is shown in Figure 20. The interface is inclined in the positive direction because of asymmetry in B_y, Equation (4). The agreement among the three software packages is excellent, except for somewhat larger slope between the two ends of the cell in the Shallow Layer model.
The velocity patterns are very similar. The large circulation pool is due to incomplete compensation of B_z at the cell center.

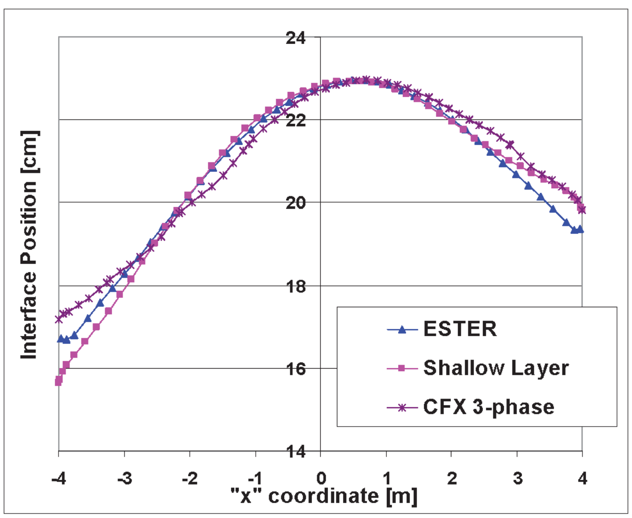

Figure 20: Comparison of calculated interface profiles for the benchmark case.

Conclusions

There are several ways to obtain correct interface shape calculations: shallow layer method, 3D floating grid method and 3D VOF method, but right boundary conditions must be used. Correct treatment of channels is important, as they release part of the pressure produced by the forces in the bath.
The agreement between the measured and calculated results is very good for Shallow Layer and ESTER models. Among VOF methods, it was shown that the 2-phase homogeneous approach is adequate to describe the simple analytical example, but in the real cell calculation a 3-phase model was needed to describe well the bath-metal interface.
Metal and bath viscosity influence the flow and the interface deformation. Constant turbulent viscosity model gave the best results. The k-ε model gave poor agreement with measured interface heights.
Finally, a benchmark case of a hypothetical cell is proposed in order to test different software packages.

References

1. J.P. Givry, "Les effets Magnétiques dans les Cuves d`électrolyse d`aluminium", *La Metallurgia Italiana n.8*, (1960), 503-509.

2. J.P. Givry, "Computer Calculation of Magnetic Effects in the Bath of Aluminum Cells", *Transactions of the Metallurgical Society of AIME – Volume 239 (AGO/1967),* 1161-1166.

3. R. Moreau and J.W. Evans, "An Analysis of the Hydrodynamic of Aluminum Reduction Cells", *Journal of Electrochemical Society - Volume 131/No10 (OCT/1984),* 2251-2259.

4. G.E. da Mota and J.E.M. Blasques, "Process Improvements to Raise the Line Current at ALBRAS", *Light Metals*, (2004), 185-190.

5. V. Potočnik, "Modeling of Metal-Bath Interface Waves in Hall-Heroult Cells Using ESTER/PHOENICS", *Light Metals*, (1989), 227-235.

6. Ch. Droste, "PHOENICS' Applications in the Aluminium Smelting Industry", *The PHOENICS Journal-Computational Fluid Dynamics and its Applications, Volume 13 No.1 (June 2000), 70-81* .

7. D. S. Severo, A. F. Schneider, E. C. V. Pinto, V. Gusberti, V. Potocnik, "Modeling Magnetohydrodynamics Of Aluminum Electrolysis Cells With Ansys And CFX", *Light Metals*, (2005), 475-480.

8. O. Zikanov, H. Sun and D. P. Ziegler, "Shallow Water Model of Flows in Hall-Héroult Cells," *Light Metals*, (2004), 445-451.

9. CFX 10.0 USER MANUAL- Solver Modelling, Multiphase Flow Modelling.

10. V. Potočnik and F. Laroche, "Comparison of Measured and Calculated Metal Pad Velocities for Different Prebake Cell Designs", *Light Metals*, (2001), 419-425.

11. S. C. Kassinos, B. Knaepen, D. Carati, "MHD Turbulence in the Presence of a Strong Magnetic Field*", Center for Turbulence Research-Procedings of the Summer Program 2002*, 191-201.

12. H. K. Versteeg and W. Malalasekera, "An Introduction to Computational Fluid Dynamics: The Finite Volume Method", Pearson-Prentice Hall, 1995, ISBN 0-582-21884-5.